Int. J. Solids Structures Vol. 22, No. 1, pp. 39–53, 1986
Printed in Great Britain.

0020–7683/86 $3.00 + .00

APPLICATION OF BODY FORCE METHOD TO THE ANALYSIS OF STRESS CONCENTRATION OF AN AXI-SYMMETRIC BODY UNDER BENDING: II. STRESS CONCENTRATION OF A CYLINDRICAL BAR WITH A SEMI-ELLIPTICAL CIRCUMFERENTIAL NOTCH UNDER BENDING

Y. MURAKAMI†, N. NODA‡ and H. NISITANI†
Department of Mechanics and Strength of Solids, Faculty of Engineering, Kyushu University, Fukuoka 812 Japan

(*Received* 19 *December* 1983; *replacement received* 22 *April* 1985)

Abstract—The stress concentration of a cylindrical bar with a semi-elliptical circumferential notch under bending is analyzed on the basis of the basic theory established in the first paper. The stress concentration factors are systematically calculated for various combination of notch dimensions. It is found that the stress concentration factors by so-called Neuber's trigonometric rule has non-conservative error of about 7% for wide range of notch depth. The stress concentration factors are illustrated in the charts so as to be used easily in designs or researches. The effect of notch shape on the stress distribution at a minimum section is also discussed from the viewpoint of the notch effect in fatigue strength of notched cylindrical bars. The error of the stress concentration factors obtained in the present analysis is less than 1% for the worst cases (very deep notch) and less than 0.1% for most cases.

1. INTRODUCTION

The stress concentration problem of a cylindrical bar with a circumferential notch (Fig. 1) is mainly used in practice for the design of shafts. It is also important with respect to the rotating bending fatigue test which has been used to investigate fatigue strength of metals. Since there have been no exact solutions of this problem, so-called Neuber's trigonometric rule[1] has been used for a long time in order to estimate stress concentration approximately. The stress concentration charts by Peterson[2] and Nisida[3], which were made on the basis of Neuber's value, have been also used. Although these charts have been used frequently in designs or researches, there have been few discussions about their accuracy. By the recent results of a strain gauge measurement[4] and analyses of finite element method[5, 6], it was suggested that Neuber's rule might have a non-conservative error. In the case of the tension problem, it was found that the maximum error was about 10%[7]. Accurate stress concentration factors and accurate stress distributions are required for the quantitative estimation of fatigue notch effect (or size effect) and for studying in detail the fatigue mechanism which is expected to be solved with the recent development of the experimental technique. Moreover, the author's review of the previous papers on fatigue notch effect has revealed that there are several data in which the fatigue limit of notched specimen σ_{w1} is smaller than the value obtained by dividing the fatigue limit of plain specimen σ_{w0} by the stress concentration factor (SCF) K_t. Such data ($\sigma_{w1} < \sigma_{w0}/K_t$) are unreasonable except for special conditions. Then the reliability of such experimental data have to be checked by the estimation based on an exact stress concentration factor K_t. Usually, σ_{w1} is fairly larger than σ_{w0}/K_t. However hard steels have a tendency that σ_{w1} is nearly equal to σ_{w0}/K_t. Therefore the unreasonable fatigue data on hard steels should be reviewed. In this paper, from these viewpoints, the calculated stress concentration factors will be compared with the values obtained by Neuber's trigonometric rule, and the effects of notch form on the stress distribution near the notch root will be also discussed. Not

† Professor.

‡ Graduate student. Current position and address: Lecturer, Department of Mechanical Engineering, Kyushu Institute of Technology, Tobata, Kitakyushu, 812 Japan.

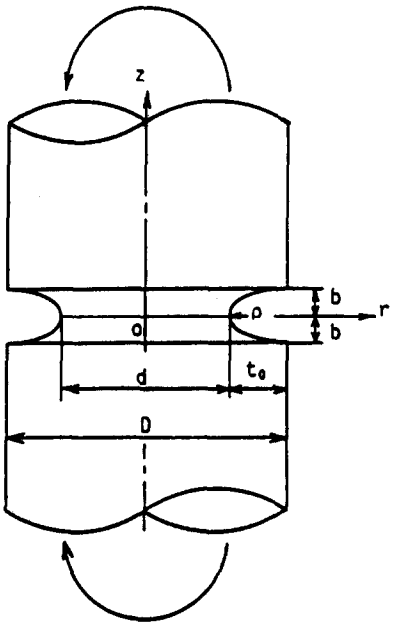

Fig. 1. A cylindrical bar with a semi-elliptical circumferential notch under bending.

only the maximum stress (factor 1) but the stress distribution (factor 2) near the notch root is significant for fatigue notch effect. The viewpoint that considers the importance of these two factors in notch effect is consistent with that of stress intensity factor in crack problems.

In the first paper[9], the basic theory of body force method was developed for the stress concentration analysis of an axi-symmetrical body under bending and it was applied to a couple of simple problems. Consequently, it was concluded that three types of ring forces in r, θ and z directions with the intensity of $\cos\phi$ or $\sin\phi$ were necessary and sufficient as the fundamental solutions to solve bending problems of an axi-symmetric body in similar manner as tension or torsion problems. In the present paper, the basic theory established in the first paper[9] is applied to the stress analysis of a cylindrical bar with a semi-elliptical circumferential notch under bending. Since a bending problem of a cylindrical bar with a circumferential notch is more difficult than tension or torsion problems, a few papers have been reported. On the analysis of semi-circular notch, Kikukawa and Sato obtained the stress concentration factors by using the strain gauge method[4] and the finite element method (FEM)[5]. Mayr, Drexler and Kuhn[10] analyzed the problem by the boundary element method (BEM). The recent development of FEM has enabled us to solve approximately almost all elasticity problems. However, FEM is unsuitable for systematic calculation of SCF K_t under various geometrical conditions. In the present paper, SCF K_t of semi-elliptical notch are systematically calculated and exact tables and charts of K_t for designs or researches are shown.

2. METHOD OF ANALYSIS

In the first paper[9], the basic theory of the body force method applied to the problems of an axi-symmetrical body under bending, and the solutions of several simple problems were shown. The problems treated in the present paper are solved in a similar manner in principle as in the first paper by using three types of ring forces as fundamental solutions. Namely, the solution of a cylindrical bar having a boundary condition in Fig. 1 can be obtained by distributing three types of fundamental solutions (in Figs. 2–4) along the boundaries which is imagined in an infinite body and is expected to become a traction-free cylindrical surface and circumferential notch. The intensities of distributed ring forces are determined from the boundary conditions. It was shown

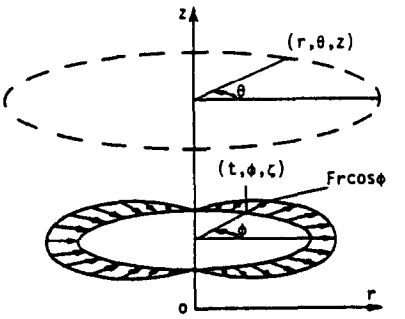

Fig. 2. A ring force with intensity cos ϕ in r-direction.

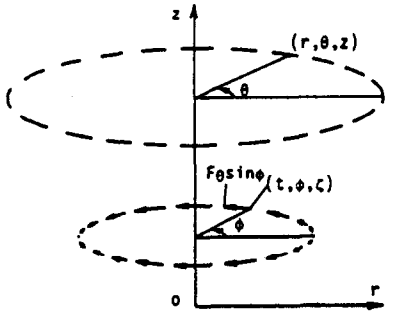

Fig. 3. A ring force with intensity sin ϕ in θ-direction.

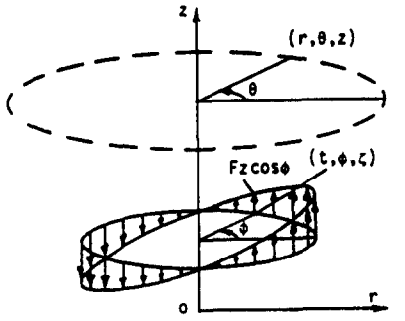

Fig. 4. A ring force with intensity cos ϕ in z-direction.

in the basic theory of the first paper[9] that only one longitudinal section for satisfying boundary conditions had to be considered and consequently the problem could be treated in a similar manner as a two-dimensional case. However, additional improvements are necessary in the distribution of body forces or the divisions of boundaries in order to obtain exact solutions in the problems of the present report, because traction-free boundary conditions must be satisfied along both the cylindrical surface and the circumferential notch.

2.1. *Boundary conditions*

The boundary conditions of the problem in Fig. 1 are as follows:

(a) $r = D/2,\ b \leq |z| \leq \infty;\ \sigma_r = \tau_{rz} = \tau_{r\theta} = 0,$

(b) along the surface of a semi-elliptical circumferential notch (n: normal direction, t: tangential direction, θ: circumferential direction); $\sigma_n = \tau_{nt} = \tau_{n\theta} = 0,$ (1)

(c) $0 \leq r \leq D/2,\ |z| = \infty;\ \sigma_z = \sigma_0 (2r/d) \cos\theta$ (Other stresses vanish.)

where, σ_0 is a constant which means the intensity of the applied bending stress. The

bending moment is loaded such that σ_z has the maximum value at $\theta = 0$, the minimum value at $\theta = \pi$ and zero at $\theta = \pi/2$ and $\theta = 3\pi/2$. σ_n is the normal stress in normal direction, $\tau_{n\theta}$ is the shear stress in meridian direction and $\tau_{n\theta}$ is the shear stress in circumferential direction at the boundary of the semi-elliptical circumferential notch. These are expressed in eqn (2) in conjunction with σ_r, σ_z, τ_{rz}, $\tau_{r\theta}$ and $\tau_{\theta z}$.

$$\begin{aligned}\sigma_n &= \sigma_r \cos^2 \psi_1 + \sigma_z \sin^2 \psi_1 + 2\tau_{rz} \sin \psi_1 \cos \psi_1 \\ \tau_{nt} &= (-\sigma_r + \sigma_z) \sin \psi_1 \cos \psi_1 + \tau_{rz} (\cos^2 \psi_1 - \sin^2 \psi_1) \\ \tau_{n\theta} &= \tau_{r\theta} \mid \cos \psi_1 \mid + \tau_{\theta z} \sin \psi_1\end{aligned} \tag{2}$$

where ψ_1 is the angle made by the r-axis and the normal direction of the semi-ellipse of the notch shape.

2.2. *Definition of the density of the body force*

The densities ρ_r, ρ_θ and ρ_z of the body force distributed in r, θ and z direction are defined in eqn (3), (4):

along the circumferential notch;

$$\rho_r \cos \psi = \frac{dF_r}{t\, d\zeta\, d\psi},\ \rho_\theta \sin \psi = \frac{dF_\theta}{t\, ds\, d\psi},\ \rho_z \cos \psi = \frac{d}{2t} \frac{dF_z}{t\, dt\, d\psi} \tag{3}$$

along the cylindrical surface;

$$\rho_r \cos \psi = \frac{dFr}{t\, d\zeta\, d\psi},\ \rho_\theta \sin \psi = \frac{dF_\theta}{t\, d\zeta\, d\psi},\ \rho_z \cos \psi = \frac{dF_z}{t\, d\zeta\, d\psi} \tag{4}$$

where dF_r, dF_θ and dF_z denote the r-, θ- and z-component of the point forces distributed along the infinitesimal curved area $t\, d\phi\, ds$ ($ds = \sqrt{(dt)^2 + (d\zeta)^2}$), and (t, ϕ, ζ) is a cylindrical coordinate of a point where point forces act. The definition of ρ_z in eqn (3) is defined considering the bending stress field $\sigma_z = \sigma_0 (2r/d) \cos \phi$.

2.3. *Method for dividing boundaries and distributing body forces*

In Fig. 5, a cylindrical surface and a troidal surface having an elliptical cross section which represents notch form are shown. We define the boundaries (the dotted line in Fig. 5) by those infinitesimally near the boundaries where the boundary conditions are to be satisfied. Body forces are distributed along these boundaries. It is difficult to determine in closed forms the body force densities which satisfy the boundary conditions completely. Therefore, the boundaries are divided and the problem is solved numerically. The values of densities of body forces, which are assumed to be constant in each division, are determined from the boundary condition at the midpoint of each division. The boundary length in z-direction O'C and O'C' (the dimension of the specimen) in Fig. 5 is determined from the condition that the calculated results virtually do not change by increasing its length. The minimum value of the length O'C and O'C' was about two times of outer diameter D. The divisions of cylindrical surface are set to be fine near the notch and coarse in proportion to the distance from the notch, that is, the boundary BC is divided into the sections, the length of which vary in a geometric series from B with the first term b and the common ratio 2 or 3. Each section is divided into a set of finer divisions. The boundary conditions of the cylindrical surface are satisfied at the midpoint of these finer divisions. On the other hand, the boundary of the semi-elliptical notch is divided concerning ψ which is a variable in the parametric equations of ellipse:

$$r = a \cos \psi + D/2, \qquad z = b \sin \psi. \tag{5}$$

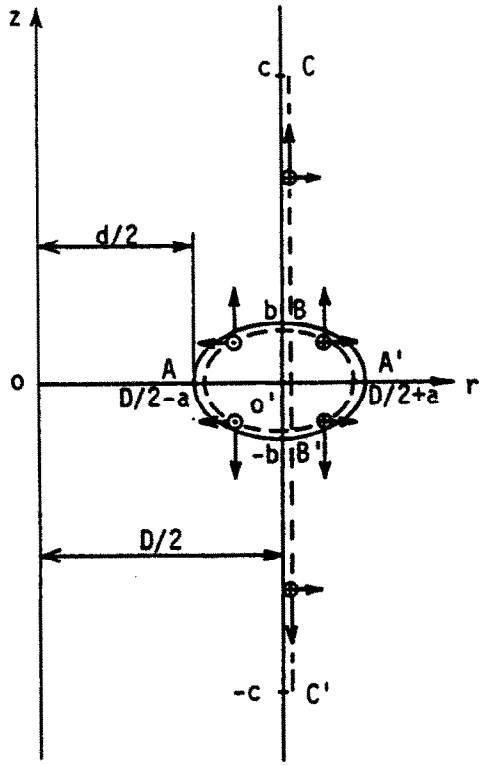

Fig. 5. A cylindrical surface CBO'B'C' and a troidal surface having an elliptical cross section ABA'B' imagined in an infinite body.

Dividing the elliptic arc AB in Fig. 5 into n_1 divisions, we number them from A to B. The pair divisions in arc AB', A'B and A'B' are numbered the same number. The interval of j-th divisions (ψ_{j_1}–ψ_{j_2}) are given by eqn (6).

$$\psi_{j_1} = \pm\frac{\pi(j-1)}{2n_1}, \quad \pi \pm \frac{\pi(j-1)}{2n_1}$$
$$\psi_{j_2} = \pm\frac{\pi j}{2n_1}, \quad \pi \pm \frac{\pi j}{2n_1} \tag{6}$$

If we call the division where the boundary conditions are to satisfy the i-th division, the coordinate of the midpoint of i-th division is given by eqn (7).

$$\psi_i = \pi - \frac{\pi}{2n_1}(i - 0.5) \tag{7}$$

In the troidal surface in Fig. 5, the densities of body forces distributed along the j-th divisions in AB, AB', A'B and A'B' are determined by satisfying the boundary conditions at the each midpoint of i-th division in AB. Body forces are applied along the arc A'B and A'B' in addition to the arc AB and AB' which should be a semi-elliptical notch, because it makes the shear stress τ_{rz} at B and B' small and consequently the boundary conditions can be satisfied easily. The positive directions of the body forces are illustrated with arrows in Fig. 5. Considering the analysis of troidal hole under bending reported in the first paper, these directions are suitable to obtain accurate results. In the case of a very deep notch, it was found that body forces distributed at BA' and B'A' had a bad effect on the numerical results, because of the great difference between the curved areas of AB, AB' and BA', B'A'. In order to cope with such cases, the form of BA'B' of the deep notch in the Fig. 5 was changed to the semi-circle with the radius b.

The division along the cylindrical surface BC are numbered from B as $j = n_1 + 1-n_1 + n_2$. The division along B'C' has the same number as BC from symmetry. Near the point B, the body force densities tend to become unbounded values because of the abrupt change of boundaries. Such a trend has a bad effect on the numerical results. In order to avoid such a effect, the linear distribution of body forces along the boundary O'B (and O'B') is added to the $(n_1 + 1)$-th division as shown in Fig. 6. Although only a body force in r-direction is shown in Fig. 6, the body forces in θ- and z-directions are also applied in the same way. In this way, we have finite body force densities at $(n_1 + 1)$-th division.

2.4. *Calculation of influence coefficients*

In this paper, the stresses induced at the midpoint of the i-th division by the distributed body force with unit density at the j-th division are called the influence coefficient. These stresses can be calculated by integrating the stresses $\sigma_r^{F_r*}-\tau_{\theta z}^{F_z*}$ due to ring forces shown in Fig. 2–Fig. 4 ($\sigma_r^{F_r*}-\tau_{\theta z}^{F_z*}$ is given in eqns (5)–(8) in the first report). Taking $\sigma_{rt}^{\rho r j}$, $\sigma_{rt}^{\rho\theta j}$ and $\sigma_{rt}^{\rho z j}$ as examples, we can write them as eqn (8), where the relation $d\zeta = (b/a)t'\, d\psi$ ($t' = t - D/2$) and $dt = (a/b)\zeta\, d\psi$ are used.

$$
\begin{aligned}
\sigma_{rt}^{\rho r j} &= \int_{\psi_{j1}}^{\psi_{j2}} \sigma_r^{F_r*} \frac{b}{a} t'\, d\psi, \quad \sigma_{rt}^{\rho\theta j} = \int_{\psi_{j1}}^{\psi_{j2}} \sigma_r^{F_\theta*} \sqrt{\left(\frac{b}{a}t'\right)^2 + \left(\frac{a}{b}\zeta\right)^2}\, d\psi, \\
\sigma_{rt}^{\rho z j} &= \int_{\psi_{j1}}^{\psi_{j2}} \sigma_r^{F_z*} \frac{2t}{d}\frac{a}{b}\zeta\, d\psi \qquad (j = 1-n_1) \\
\sigma_{rt}^{\rho r j} &= \int_{z_{j1}}^{z_{j2}} \sigma_r^{F_r*}\, d\zeta, \quad \sigma_{rt}^{\rho\theta j} = \int_{z_{j1}}^{z_{j2}} \sigma_r^{F_\theta*}\, d\zeta, \\
\sigma_{rt}^{\rho z j} &= \int_{z_{j1}}^{z_{j2}} \sigma_r^{F_z*}\, d\zeta \quad (j = n_1 + 1-n_1 + n_2)
\end{aligned}
\tag{8}
$$

where $(\psi_{j1}-\psi_{j2})$ is the interval of j-th division in the circumferential notch and $(z_{j1}-z_{j2})$ is that in the cylindrical surface. The integrations in eqn (8) are performed numerically using Simpson's rule. The boundary stresses due to body forces at the circumferential notch are expressed in the forms of $\sigma_{nti}^{\rho r j}$, $\tau_{nti}^{\rho r j}$, . . . $\rho_{n\theta i}^{\rho z j}$ by substituting the stresses $\sigma_{rt}^{\rho r j}$, $\sigma_{zt}^{\rho r j}$, $\tau_{rzi}^{\rho r j}$ . . . . into eqn (2).

2.5. *Determination of body force densities*

The body force densities are determined by solving the following $3(n_1 + n_2)$ linear equations.

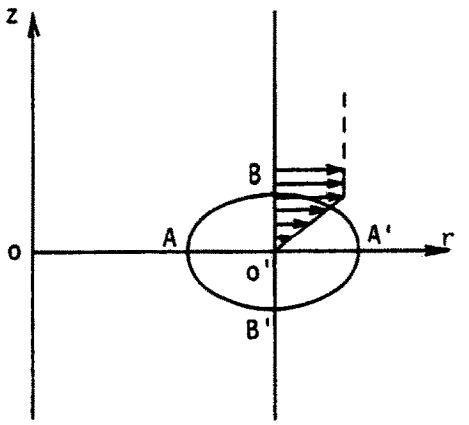

Fig. 6. Distributing method of body forces on O'B.

$$\sum_{j=1}^{n_1+n_2} (\rho_{rj}\sigma_{ni}^{\rho rj} + \rho_{\theta j}\sigma_{ni}^{\rho\theta j} + \rho_{zj}\sigma_{ni}^{\rho zj}) + \sigma_0 \frac{2r_i}{d} \sin^2 \psi_1 = 0 \qquad (i = 1\text{–}n_1)$$

$$\sum_{j=1}^{n_1+n_2} (\rho_{rj}\tau_{n\theta i}^{\rho rj} + \rho_{\theta j}\tau_{n\theta i}^{\rho\theta j} + \rho_{zj}\tau_{n\theta i}^{\rho zj}) + \sigma_0 \frac{2r_i}{d} \sin \psi_1 \cos \psi_1 = 0 \qquad (i = 1\text{–}n_1)$$

$$\sum_{j=1}^{n_1+n_2} (\rho_{rj}\tau_{nzi}^{\rho rj} + \rho_{\theta j}\tau_{nzi}^{\rho\theta j} + \rho_{zj}\tau_{nzi}^{\rho zj}) = 0 \qquad (i = 1\text{–}n_1) \tag{9}$$

$$\sum_{j=1}^{n_1+n_2} (\rho_{rj}\sigma_{ri}^{\rho rj} + \rho_{\theta j}\sigma_{ri}^{\rho\theta j} + \rho_{zj}\sigma_{ri}^{\rho zj}) = 0 \qquad (j = n_1 + 1\text{–}n_1 + n_2)$$

$$\sum_{j=1}^{n_1+n_2} (\rho_{rj}\tau_{rzi}^{\rho rj} + \rho_{\theta j}\tau_{rzi}^{\rho\theta j} + \rho_{zj}\tau_{rzi}^{\rho zj}) = 0 \qquad (j = n_1 + 1\text{–}n_1 + n_2)$$

$$\sum_{j=1}^{n_1+n_2} (\rho_{rj}\tau_{r\theta i}^{\rho rj} + \rho_{\theta j}\tau_{r\theta i}^{\rho\theta j} + \rho_{zj}\tau_{r\theta i}^{\rho zj}) = 0 \qquad (j = n_1 + 1\text{–}n_1 + n_2)$$

where r_i is the r-coordinate at the midpoint of the i-th division. Once the body force densities are determined, the stresses at an arbitrary point can easily be calculated by using the body force densities and the stresses at the point due to unit body force density which can be determined from eqn (8) in the same manner as the influence coefficients.

2.6. *Fundamental equations*

The fundamental equations of stress field due to ring forces shown in Fig. 2–Fig. 4, which are necessary for calculating $\sigma_{ni}^{\rho rj}$, $\sigma_{ni}^{\rho\theta j}$, . . . in eqn (9), are given by eqns (5)–(8) in the first paper[9]. These are not written in the present paper to avoid overlap.

3. NUMERICAL RESULTS AND DISCUSSION

A computer program for the analysis of a cylindrical bar with a semi-elliptical circumferential notch was coded on the basis of the procedures for the numerical analysis described in Section 2. The integral in eqn (8) was numerically performed by Sympson's rule with 10 dividing numbers. When the body forces are distributed along the division under consideration of boundary condition (i.e. $i = j$), or when the maximum stresses at the end of major axis must be calculated, the numbers of divisions for numerical integral was increased by 10-times as that of other case. Stress concentration factors (SCF) K_t were determined from the maximum stress σ_{max} and the nominal stress σ_n calculated from the bending moment M which were obtained by integrating the stresses $\sigma_z(r)$ at the minimum section OA in Fig. 5. Therefore, it follows:

$$M = 4 \int_0^{d/2} \int_0^{\pi/2} \sigma_z(r) r^2 \cos^2 \theta \, d\theta \, dr$$

$$= \pi \int_0^{d/2} \sigma_z(r) r^2 \, dr \tag{10}$$

$$K_t = \frac{\sigma_{max}}{\sigma_n}, \qquad \sigma_n = \frac{32M}{\pi d^3}. \tag{11}$$

In the subsequent sections, SCF obtained in this way are tabulated and illustrated with the attention to the effects of two parameters; the notch depth t_0 and the notch root

radius ρ. t_0 and ρ are expressed with the major and minor axis of a semi-ellipse (a and b) as $t_0 = a$ and $\rho = b^2/a$. Poisson's ratio is assumed to be 0.3.

3.1. *Variation of stress concentration factors with increasing dividing numbers* n_1 *and* n_2

Table 1 shows examples of stress concentration factors calculated for various dividing numbers n_1 (notch) and n_2 (cylindrical surface). The symbol ∞_{6-8} means the extrapolated value using the results for $n_1 = 6$ and 8. Although the numbers of divisions n_1 and n_2 were naturally restricted by the computer capacity, the accuracy of the numerical results discussed below were checked in the same manner as Table 1. The authors assure the error in the present analysis is less than 1% for the worst cases, and less than 0.1% for most cases.

3.2. *SCF of semi-circular circumferential notch*

In Table 2, SCFs of semi-circular notch are compared with the results by other researches. Neuber's trigonometric rule has about 5% error in case of a shallow notch. The experimental value of Kikukawa and Sato[4], which were obtained by strain gauge measurement, are in good agreement with the present results. SCFs in Table 2 are plotted in Fig. 7. As $2\rho/D \to 0$, SCF of semi-circular notch approaches the value $K_t = 3.065$[11] which is SCF of a semi-circular notch in a semi-infinite plate under tension. And as $2\rho/D \to 1$, SCF approaches the value $K_t = 1$. In Fig. 7, the numerical results by Mayr, Drexler and Kuhn[10] are also plotted. Their results tend to have large error for the large value of $2\rho/D$.

Table 1. Variation of stress concentration factors with increasing dividing numbers n_1 and n_2($\nu = 0.3$, $t_0 = a$, $\rho = b^2/a$)

	$2\rho/D = 0.03$			$2\rho/D = 0.2$		
$2t_0/D$	n_1	n_2	Kt	n_1	n_2	Kt
0.3	6	36	3.793850	6	30	1.787203
	8	42	3.794725	8	40	1.786952
	12	72	3.795277	12	60	1.786737
	∞_{6-8}		3.797	∞_{6-8}		1.786
	∞_{8-12}		3.796	∞_{8-12}		1.786
0.7	8	40	2.659077	8	32	1.380065
	12	60	2.662158	12	48	1.382803
	16	80	2.663327	16	64	1.384048
	∞_{8-12}		2.668	∞_{8-12}		1.388
	∞_{12-16}		2.667	∞_{12-16}		1.388

Table 2. Stress concentration factors of a cylindrical bar with a semi-circular circumferential notch under bending ($\nu = 0.3$)

$2\rho/D$	Present analysis	[4]	[5]	Neuber
0.02	2.877	—	—	2.82
0.03	2.790	—	—	2.73
0.05	2.630	—	—	2.56
0.1	2.306	—	—	2.21
1/9	2.245	2.26	2.27	2.15
4/29	2.112	2.13	—	2.01
0.2	1.858	1.86	1.87	1.77
0.3	1.575	—	—	1.53
1/3	1.504	1.50	1.53	1.47
0.4	1.390	—	—	1.37
0.5	1.269	1.27	1.29	1.26
0.6	1.183	—	—	1.18
2/3	1.139	1.14	—	1.14
0.8	1.072	—	—	1.07
0.9	1.032	—	—	1.03

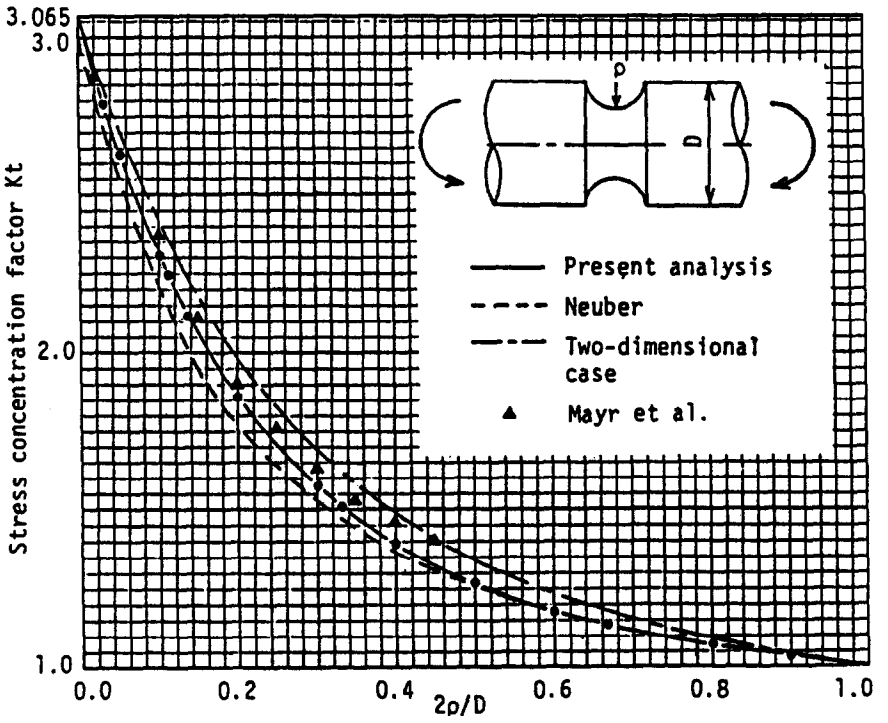

Fig. 7. Stress concentration factor of a cylindrical bar with a semi-circular circumferential notch under bending (ν = 0.3).

3.3. *SCF of semi-elliptical circumferential notch*

In Table 3, SCFs of semi-elliptical notch and corresponding values by Neuber's trigonometric rule are shown. The present results in Table 3 were obtained by the extrapolation from the results of n_1 = 8–16 and n_2 = 40–80. By systematic calculation shown in Table 3 and Fig. 8, it may be concluded that Neuber's trigonometric rule has about 7% of non-conservative error for the wide range of notch depth. The charts of SCF are also shown in different way in Figs. 9 and 10, where the abscissa is $2\rho/D$. Using these charts (Fig. 8–10), SCF K_t not calculated in the present paper will be estimated.

3.4. *Stress distribution near notch root*

Figs. 11–13 show the stress distributions near the root of notch at a minimum section. The ordinates represents the dimensionless stress σ_z/σ_{max}, where σ_{max} denotes the maximum stress at the root of notch. The abscissa represents the dimensionless distance x/ρ from the notch root. We find from these figures that the dimensionless stress distributions near the root of a notch are approximately independent of the variation of notch depth, if the notch root radius is kept constant.

Concerning the study of notch effect or size effect in rotating bending fatigue test, Nisitani[12] proposed a method to determine the fatigue limit of the notched specimen of an arbitrary size from the experimentally verified facts; (1) the root radius of a notch at the branch point ρ_0 is a material constant and independent of the notch depth, and (2) the maximum stress amplitude ($K_f\sigma_{w1}$) at the notch root at the fatigue limit based on crack initiation is a unique function of the stress gradient at the notch root. And then, he pointed out that the notch root radius ρ was a most important controlling factor in the notch effect (or size effect), because the stress distribution near the notch root was almost completely determined by the notch root radius. In his paper[12], this was discussed using Neuber's solutions. As seen in Figs. 11–13, his finding has been confirmed more accurately and concretely by the present analysis.

Table 3. Stress concentration factors of a cylindrical bar with a semi-elliptical circumferential notch under bending ($\nu = 0.3$, $t_0 = a$, $\rho = b^2/a$)

	$2\rho/D = 0.02$		$2\rho/D = 0.03$		$2\rho/D = 0.05$		$2\rho/D = 0.1$		$2\rho/D = 0.2$		$2\rho/D = 0.5$		$2\rho/D = 1.0$	
$2t_0/D$	Present analysis	Neuber	Present analysis	Neuber	Present analysis	Neuber	Present analysis	Neuber	Present analysis	Neuber	Present analysis	Neuber	Present analysis	Neuber
0.02	2.877	2.82	2.511	2.48	2.147	2.13	1.785	1.78	1.532	1.53	1.311	1.31	1.202	1.19
0.05	3.708	3.56	3.169	3.06	2.630	2.56	2.099	2.05	1.728	1.69	1.407	1.37	1.250	1.22
0.1	4.324	4.06	3.648	3.45	2.974	2.83	2.306	2.21	1.845	1.77	1.450	1.40	1.262	1.22
0.2	4.667	4.33	3.893	3.64	3.124	2.95	2.375	2.25	1.858	1.77	1.427	1.38	1.232	1.21
0.3	4.57	4.28	3.796	3.58	3.035	2.88	2.293	2.19	1.786	1.72	1.375	1.35	1.198	1.19
0.4	4.31	4.10	3.579	3.42	2.868	2.75	2.164	2.09	1.695	1.65	1.320	1.31	1.167	1.16
0.5	3.98	3.83	3.308	3.20	2.656	2.58	2.017	1.97	1.596	1.57	1.269	1.26	1.139	1.14
0.6	3.59	3.50	3.007	2.93	2.424	2.37	1.860	1.83	1.494	1.48	1.218	1.21	1.112	1.11
0.7	3.18	3.10	2.667	2.61	2.168	2.12	1.692	1.67	1.388	1.38	1.166	1.16	1.085	1.09
0.8	2.68	2.62	2.27	2.22	1.87	1.84	1.499	1.48	1.272	1.26	1.113	1.11	1.058	1.06
0.9	2.04	1.99	1.77	1.73	1.51	1.48	1.27	1.26	1.14	1.14	1.058	1.06	1.028	1.03

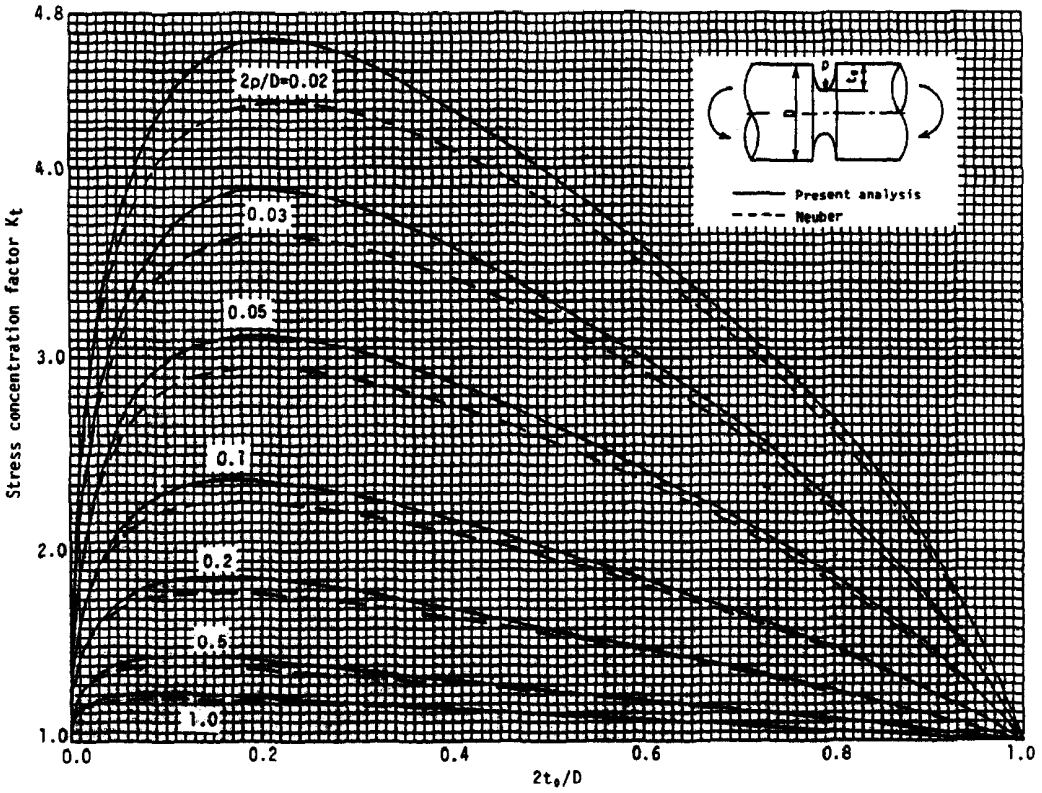

Fig. 8. Stress concentration factor of a cylindrical bar with a semi-elliptical circumferential notch under bending ($\nu = 0.3$, $t_0 = a$, $\rho = b^2/a$).

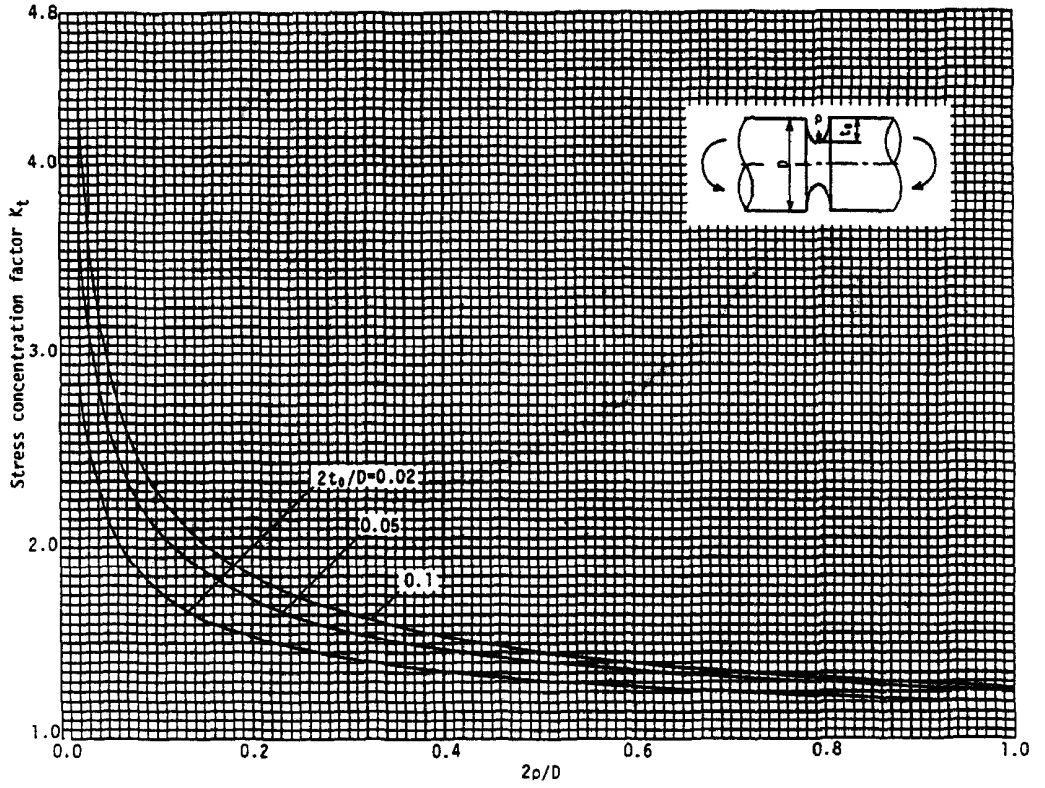

Fig. 9. Stress concentration factor of a cylindrical bar with a semi-elliptical circumferential notch under bending.

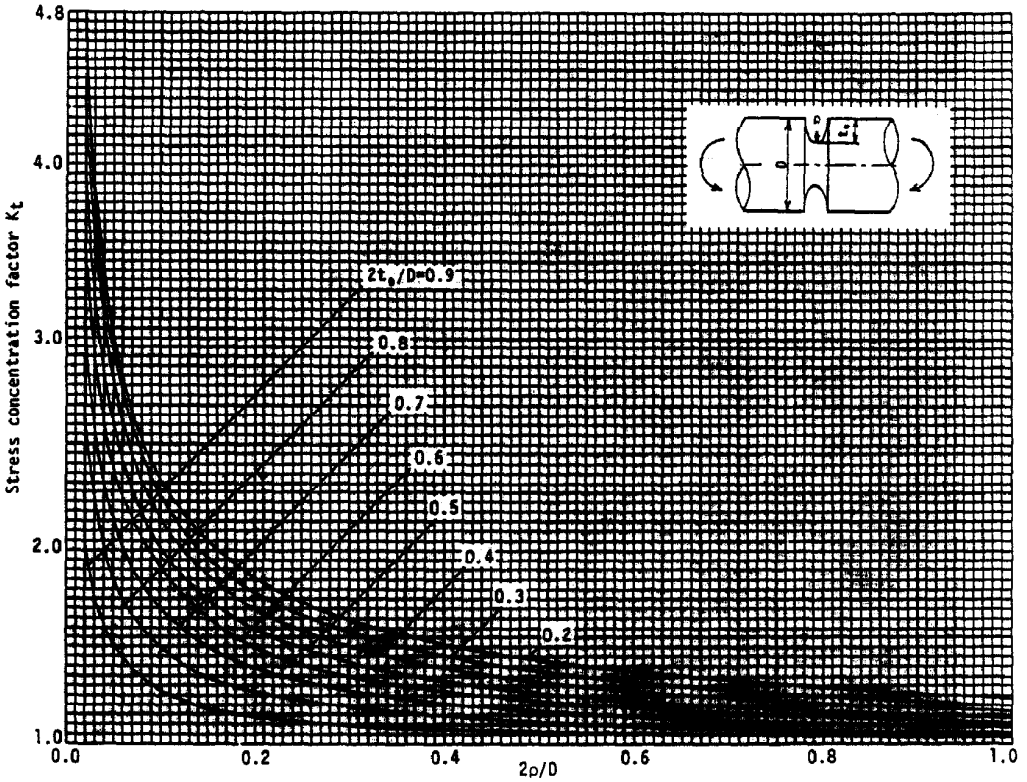

Fig. 10. Stress concentration factor of a cylindrical bar with a semi-elliptical circumferential notch under bending.

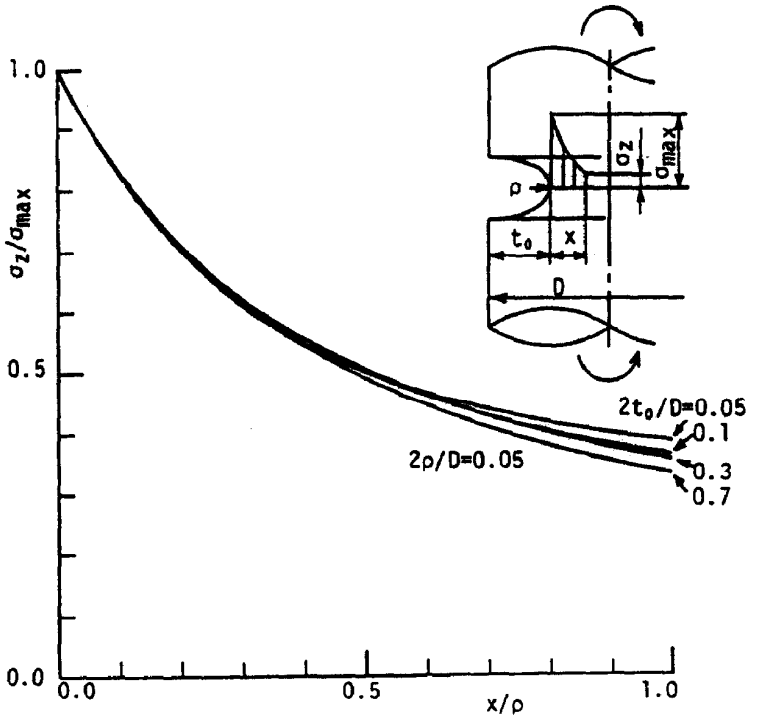

Fig. 11. Stress distribution near the root of notch (in case of a sharp notch).

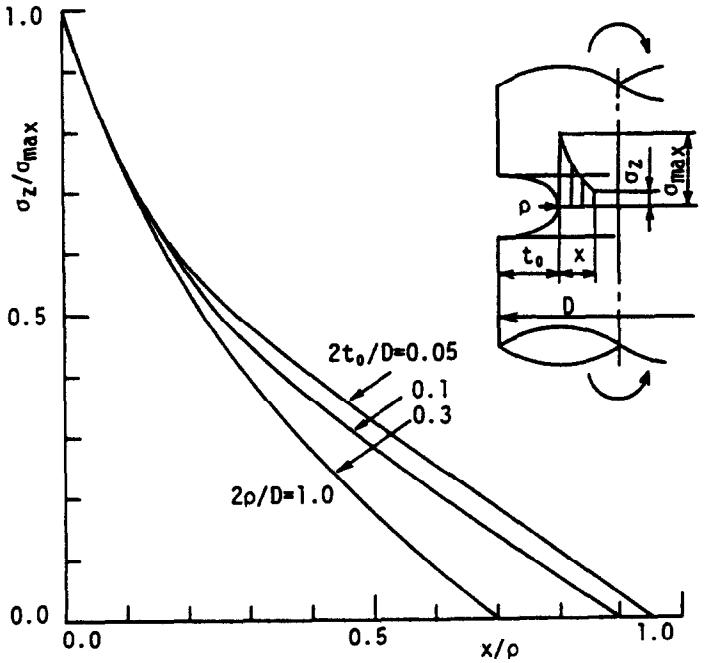

Fig. 12. Stress distribution near the root of notch.

3.5. *Review of the experimental data about notch effect in the rotating bending fatigue test*

As already described in Section 1, in the previous studies about the fatigue notch effect, there are several data in which the fatigue limit of a notched specimen σ_{w1} is smaller than the value of the fatigue limit of a plane specimen σ_{w0} divided by SCF K_t, i.e. $\sigma_{w1} < \sigma_{w0}/K_t$. Not only the maximum stress but also the stress gradient is a important factor controlling the crack initiation at the root of the notch. From this viewpoint, these data showing $\sigma_{w1} < \sigma_{w0}/K_t$ are unreasonable, because the stress gradient

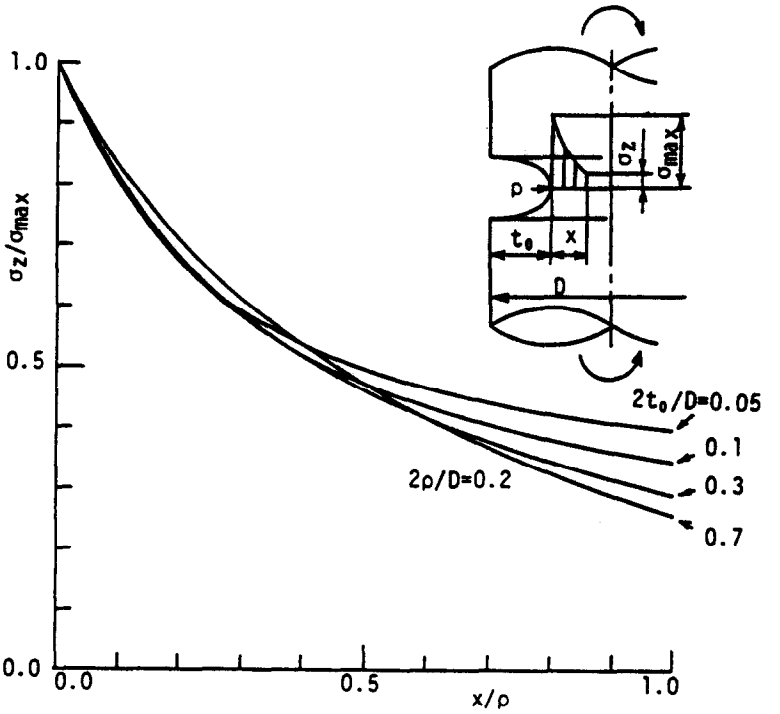

Fig. 13. Stress distribution near the root of notch (in case of a blunt notch).

Table 4. Review of the experimental data about notch effect in the rotating fatigue test (σ_{w0}, σ_{w0}: kgf/mm^2)

	$2\rho/D$	$2t_0/D$	SCF used in the experiment K_t'	SCF obtained by authors K_t	σ_{w0}	σ_{w0}/K_t'	σ_{w0}/K_t	σ_{w1}	material
Nishioka *et al.*[13]	0.04	1/3	3.1	3.282	43	13.9	13.1	13	9% nickel steel
	"	"	"	"	56	18.1	17.1	17	
	"	"	"	"	45	14.5	13.7	14	
	"	"	"	"	60	19.4	18.3	18	
Shimizu *et al.*[14]	1/15	1/3	2.20	2.651	50	22.7	18.9	20	induction hardened 0.15% carbon steel

of the notched specimen is steeper than that of the plane specimen with the same minimum cross section. In the following, several experimental values are reviewed using an accurate SCF K_t obtained in the present paper.

Table 4 shows several examples of experimental data showing $\sigma_{w1} < \sigma_{w0}/K_t$. The experiment by Nishioka, Hirakawa and Toyama[13] was carried out on the 9% nickel steel at room- or low-temperature. If we use Neuber's value $K_t' = 3.1$ in order to estimate the stress concentrations of the notched specimens, these experimental data seem to be unreasonable. However, if we use SCF $K_t = 3.282$ obtained by the present analysis, they can be understood reasonable. We must consider that the fatigue limits were determined by $1 kgf/mm^2$ step in this experiment. The experiment of Shimizu, Nakamura and Kunio[14] was carried out on the induction-hardened 0.15% carbon steel. In this case too, if we use $K_t = 2.651$ obtained by the present analysis, σ_{w1} becomes larger than σ_{w0}/K_t. Other experimental data of previous researches are also reviewed and it was found that there were some cases where the correct Neuber's value was not necessarily used because of reading error in the charts. Therefore, it should be noticed that the exact discussion is not likely to be done by using Neuber's SCF.

4. CONCLUSION

Since there were no exact solutions for the problem of a cylindrical bar with a circumferential notch under bending, the approximate stress concentration factors (SCF) by Neuber's trigonometric rule have been used for a long time for designs or researches. It has been accepted generally that the error of Neuber's SCF is not so large. There has been few discussions about the accuracy of Neuber's SCF. In the present study, the problem was solved numerically on the basis of the basic theory established in the first paper. Although solutions were obtained numerically, they have a high accuracy and may be considered to the exact solutions for the practical use. The conclusions are summarized as follows:

(1) SCF of a cylindrical bar with a semi-elliptical circumferential notch under bending were systematically calculated for various combination of notch dimensions. It was found that Neuber's trigonometric rule has non-conservative error for wide range of notch depth. The error of the present analysis is less than 1% for the worst cases and less than 0.1% for most cases.
(2) The stress concentration factors were illustrated in the charts so as to be used easily in designs or researches.
(3) The effect of notch form on the stress distribution near notch root was investigated. The stress distribution near notch root is controlled mainly by the root radius of a notch and is independent of other dimensions. This is the key point to understand notch effect or size effect[12].
(4) As $2\rho/D \to 0$, SCF of the semi-circular notch approaches the value $K_t = 3.065$[11], which is SCF of a semi-circular notch in a semi-infinite plate under

tension. As $2\rho/D \to 1$, SCF approaches the value $K_t = 1$. The experimentally determined values by Kikukawa and Sato[4] are in good agreement with the present results.

(5) In the previous studies about the fatigue notch effect, there are some data indicating $\sigma_{w1} < \sigma_{w0}/K_t'$. Apparently, they are unreasonable values. However, if they are reconsidered by accurate SCF K_t obtained in the present paper, some of them become $\sigma_{w1} > \sigma_{w0}/K_t$ and are regarded reasonable.

REFERENCES

1. H. Neuber, *Kerbspannungslehre*. Springer-Verlag, Berlin (1957).
2. R. E. Peterson, Stress concentration design factors. John-Wiley & Sons, New York (1962).
3. M. Nisida, *Stress Concentration* (in Japanese), Morikitashuppan, Tokyo (1972).
4. M. Kikukawa and Y. Sato, Stress concentration in notched bars (2nd Report, U-grooved Shafts). *Trans. Japan. Soc. Mech. Engrs* (in Japanese) **38**, 1673–1680 (1972).
5. Y. Sato, M. Kikukawa and T. Matsui, Stress concentration in notched bars (4th Report, Finite Element Analysis of Semicircular Shafts). *Trans. Japan Soc. Mech. Engrs* (in Japanese) **42**, 3701–3709 (1976).
6. H. Miyamoto, Calculation of stress concentration by finite element method. *J. Japan Soc. Precis. Engng* (in Japanese) **35**, 609–623 (1969).
7. Y. Murakami, N. Noda and H. Nisitani, The analysis of stress concentration of a cylindrical bar with a semi-elliptical circumferential notch under tension. *Trans. Japan Soc. Mech. Engrs* (in Japanese) **47**, 1194–1205 (1981).
8. H. Nisitani and Y. Murakami, Method of analysis of crack tip stress intensity factor. *J. Japan Soc. Mech. Engrs* (in Japanese) **75**, 1081–1090 (1972).
9. Y. Murakami, N. Noda and H. Nisitani, Application of body force method to the analysis of stress concentration of an axi-symmetric body under bending: I. Basic theory and application to several simple problems. *I. J. Solids Structures* **21**, 000–000 (1985).
10. M. Mayr, W. Drexler and G. Kuhn, A semianalytical boundary integral approach for axisymmetric elastic bodies with arbitrary boundary conditions. *I. J. Solids Structures* **16**, 863–871 (1980).
11. M. Isida, On the tension of the strip with semicircular notches. *Trans. Japan Soc. Mech. Engrs* (in Japanese) **19**, 5–10 (1953).
12. H. Nisitani, Effects of size on the fatigue limit and the branch point in rotary bending tests of carbon steel specimens. *Bull Japan Soc. Mech. Engrs* **11**, 947–957 (1968).
13. K. Nisioka, K. Hirakawa and K. Toyama, Effects of Anisotropy on Fatigue Strength. *Proc. 13th Symp. on Fatigue* (in Japanese), *Society of Materials Science*, Japan, 84–88 (1980).
14. M. Shimizu, H. Nakamura and T. Kunio, An experiment on the effect of induction hardening on fatigue strength (Report 9, On the fatigue crack initiation and its propagation in the low carbon steel notched specimen induction hardened). *Trans Japan Soc. Mech. Engrs* (in Japanese) **34**, 230–236 (1968).